Behavioral Crowds: Modeling and Monte Carlo Simulations Toward Validation[☆]

N. Bellomo[a], L. Gibelli[b]

[a]*Department of Mathematics, Faculty Sciences, King Abdulaziz University, Jeddah, Saudi Arabia*
Address: Politecnico di Torino, 10129 Torino, Italy
[b]*Department of Mathematica Sciences, Politecnico di Torino*
Corso Duca degli Abruzzi 24, 10129 Torino, Italy

Abstract

A mesoscopic model of behavioral crowds is developed within the framework of the kinetic theory for active particles. An analytic long-time equilibrium solution is obtained which gives a fundamental density-velocity diagram consistent with the empirical evidence. Numerical simulations based on a Monte Carlo particle method show that the proposed model has the capability to qualitatively depict emerging behaviors and to provide a realistic description of the crowd dynamics in complex evacuation scenarios.

Keywords: Active particles, behavioral dynamics, Monte Carlo particle method, fundamental diagram, lanes formation, evacuation time

PACS: 89.20.-a, 89.75.-k, 05.10.-a, 02.70.Uu

[☆]This paper is dedicated to Tayfun Tezduyar on the occasion of his 60th birthday.

Email addresses: nicola.bellomo@polito.it (N. Bellomo), livio.gibelli@polimi.it (L. Gibelli)

1. Introduction

Crowd dynamics has received a growing attention in the last two decades not only for its theoretical interest but also for the potential societal benefits. A realistic modeling of the walker's behavior can permit, for instance, to improve the design of buildings, aircraft and ships with respect to their safety in the event of an emergency evacuation and/or to understand how to control crowd movements in different situations.

It is well known that the modeling of crowd dynamics can be developed at three representation scales, namely microscopic, macroscopic, and mesoscopic [1]. A valuable reference concerning, modeling, mathematical problems, and applications related to the microscopic and macroscopic scales is provided by Ref. [2]. Microscopic models assume that the dynamics of the crowd emerges from the movement of individuals [3]. The state of the crowd is thus defined by specifying position and velocity of individuals and the dynamics is predicted on the basis of rules by which interactions between individuals are modeled. In contrast the focus of the macroscopic models is on the crowd as a whole [4]. Accordingly, the state of the crowd is described with aggregate observables, such as density and velocity, and the dynamics is governed by balance equations for mass and/or momentum closed through phenomenological assumptions. Mesoscopic models are situated at an intermediate level between these two scales [5]. The state of the crowd is described by means of a probability distribution function over the microscopic state of individuals, namely position and velocity, while an additional internal variable is introduced to depict their heterogeneous behavioral strategy. Interactions between individuals are modeled at the micro-scale, while

the aggregate observables are obtained by weighted moments of the aforesaid probability distribution.

A critical analysis of the advantages and drawbacks of the different scales selected for the modeling approach are discussed in the Ref. [1], where it is concluded that the present state of the art does not yet allow well defined hallmarks to support an optimal choice. Microscopic models are shown to provide realistic results. However, keeping track of the individual state of each walker leads to numerical simulations which are computationally demanding. Moreover, the results obtained from such approach may not be easily interpreted in the absence of a higher level model. Indeed it may be difficult, or nearly impossible, to use data from microscopic observations to infer the crowd behavior in a different but similar situation. Macroscopic models are appealing in that they allow to investigate complex dynamics which otherwise would be very difficult to deal with. An example is the pedestrian flows coupled with vehicular traffic networks studied in Ref. [6]. On the other hand, the heterogeneous behavior of walkers gets lost in the averaging process needed to their derivation and therefore macroscopic models totally disregard this important feature. Mesoscopic models have the potential of providing the crucial ingredients towards an accurate description of a crowd viewed as a living, hence complex, system but, in order to achieve such an objective, further developments are needed both from the modeling and computational standpoints.

In the present paper, a mesoscopic model is proposed based on two previous contributions to the modeling of crowd dynamics by the kinetic theory of active particles, Refs. [7, 8], where the former proposes a modeling approach

in unbounded domains, while the latter takes into account interactions with walls. More specifically, the model proposed in Ref. [8] is revisited so as to simplify its mathematical formulation and, at the same time, better reproduce the empirical evidence.

The validation of crowd models against reality is a challenging topic that is poorly treated in the literature, with a few exceptions such as, for instance, Refs. [9–11]. The empirical evidence is quite limited to develop a detailed comparison and, in addition, most of the data are available at the macroscopic scale, while the modeling process needs a detailed understanding of the microscopic dynamics. Therefore a strategy should be elaborated to exploit the available data at the best of the panorama they offer. In the present study, we assess the ability of the proposed model to reproduce the density-velocity diagram in steady flow conditions and to depict some collective emerging behaviors which are observed by experiments, namely the self-organized behaviors which leads to the creation of lanes in streets and the increasing of evacuation time in panic conditions.

The presentation is proposed as follows. In Section 2, the mathematical formulation of the crowd mesoscopic model is described. In Section 3, an analytic long-time equilibrium solution is obtained which is shown to provide a fundamental density-velocity diagram consistent with the empirical evidence. In Section 4, after a brief introduction of the Monte Carlo particle method of solution, it has been numerically assessed that the proposed model has the capability to reproduce self-organized collective crowd behaviors which are empirically observed. In Section 5, conclusions and future research directions are presented.

2. Mesoscopic models of social crowd

Let us consider a crowd in a venue $\mathcal{S}$. The crowd can be subdivided into n different groups of persons which develop their own strategy, such as walking toward different targets. We refer to these groups as functional subsystems (FSs). The state of the overall system is described by the one-particle distribution functions $f_i = f_i(t, \boldsymbol{x}, \boldsymbol{v})$ with $i = 1, \ldots, n$, which are such that $f_i(t, \boldsymbol{x}, \boldsymbol{v})\, d\boldsymbol{x}\, d\boldsymbol{v}$ denotes the number of walkers of the i-th FS whose state, at time t, is in the elementary volume of the space of the microscopic states $[\boldsymbol{x}, \boldsymbol{x} + d\boldsymbol{x}]$ and $[\boldsymbol{v}, \boldsymbol{v} + d\boldsymbol{v}]$ with $\boldsymbol{x} \in \mathcal{S}$ and $\boldsymbol{v} \in \mathcal{V} := \{\boldsymbol{v} : \|\boldsymbol{v}\| < \xi_{\text{LIM}}\}$, where ξ_{LIM} is the limit velocity that a fast walker can reach in the free flow condition.

Macroscopic quantities can be computed by velocity weighted moments of the distribution function. As an example, density and the mean velocity are given by

$$\rho_i(t, \boldsymbol{x}) = \int_{D_v} f_i(t, \boldsymbol{x}, \boldsymbol{v})\, d\boldsymbol{v} \quad \text{and} \quad \boldsymbol{\xi}_i(t, \boldsymbol{x}) = \frac{1}{\rho(t, \boldsymbol{x})} \int_{D_v} \boldsymbol{v}\, f_i(t, \boldsymbol{x}, \boldsymbol{v})\, d\boldsymbol{v}. \tag{1}$$

Global expressions are obtained by summing over the index labeling the FSs, that is

$$\rho(t, \boldsymbol{x}) = \sum_{i=1}^{n} \rho_i(t, \boldsymbol{x}) \quad \text{and} \quad \boldsymbol{\xi}(t, \boldsymbol{x}) = \sum_{i=1}^{n} \boldsymbol{\xi}_i(t, \boldsymbol{x}). \tag{2}$$

The derivation of the mathematical structure used in the present work refers to the theory reviewed in Ref. [5] where walkers are viewed as active particles and interactions are modeled by theoretical tools of stochastic game theory. The balance in the elementary volume of the phase space between the inlet and outlet fluxes due to the movement of the walkers in the space

and their mutual interactions gives

$$(\partial_t + \boldsymbol{v} \cdot \nabla_{\boldsymbol{x}})\ f_i(t, \boldsymbol{x}, \boldsymbol{v}) = \\ = \eta_0 \left[\int_{\mathcal{S}\times\mathcal{V}} \mathcal{A}[\rho, \boldsymbol{\xi}](\boldsymbol{v}_* \to \boldsymbol{v}) f_i(t, \boldsymbol{x}, \boldsymbol{v}_*)\, d\boldsymbol{v}_* - f_i(t, \boldsymbol{x}, \boldsymbol{v}) \right], \quad (3)$$

where η_0 is the interaction rate between walkers and $\mathcal{A}$ is the transition probability density which models the decision process based on which walkers modify their velocity. In Eq. (3), square brackets have been used to denote the functional dependence of the transition probability density from the local mean density and velocity. Therefore, in spite of its linear appearance, the proposed crowd model is a strongly nonlinear set of integro-differential equations.

The interaction rate is assumed to be constant while the main features of the the transition probability density are summarized in Table 1. More specifically, following Ref. [8], $\mathcal{A}$ is supposed to encompasses the effects of both interactions between walkers, $\mathcal{C}$, and between walkers and wall, $\mathcal{B}$, that is

$$\mathcal{A}[\rho, \boldsymbol{\xi}]\,(\boldsymbol{v}_* \to \boldsymbol{v}) = \mathcal{B}(\tilde{\boldsymbol{v}} \to \boldsymbol{v}) \mathcal{C}[\rho, \boldsymbol{\xi}](\boldsymbol{v}_* \to \tilde{\boldsymbol{v}}), \quad (4)$$

where $\mathcal{C}$ is assumed to depend on the local density and mean velocity of the crowd. The transition probability densities $\mathcal{B}$ and $\mathcal{C}$ are described in detail in Subsections 2.1 and 2.2, respectively.

2.1. Modeling interactions between walkers

Interactions between walkers are assumed to modify their dynamics firstly by changing the direction of movement and, afterwards, by modifying the speed

$$\mathcal{C}[\rho, \boldsymbol{\xi}](\boldsymbol{v}_* \to \tilde{\boldsymbol{v}}) = \mathcal{C}_2[\rho, \boldsymbol{\xi}](v_* \to \tilde{v}) \mathcal{C}_1[\rho, \boldsymbol{\xi}](\theta_* \to \tilde{\theta}) \quad (5)$$

	Condition	*Transition*	*Probability*
Interactions	$\forall\, \theta_*$	$\theta_* \to \tilde{\theta} = \theta^{(p)}[\rho, \boldsymbol{\xi}]$	1
	$v_* \leq \xi$	$v_* \to \tilde{v} = \xi + \gamma(1 - \tilde{\rho_p}[\rho, \boldsymbol{\xi}])(\gamma\xi_{\text{LIM}} - \xi)$	$\gamma(1 - \tilde{\rho_p}[\rho, \boldsymbol{\xi}])$
		$v_* \to \tilde{v} = v_*$	$1 - \gamma(1 - \tilde{\rho_p}[\rho, \boldsymbol{\xi}])$
	$v_* > \xi$	$v_* \to \tilde{v} = \xi - \tilde{\rho_p}[\rho, \boldsymbol{\xi}]\xi$	$(1 - \gamma C)\tilde{\rho_p}[\rho, \boldsymbol{\xi}]$
		$v_* \to \tilde{v} = v_*$	$1 - (1 - \gamma C)\tilde{\rho_p}[\rho, \boldsymbol{\xi}]$
Boundary	$d_* < d_w$	$\tilde{\theta} \to \theta = \theta^{(w)}$ $\tilde{v} \to v = \tilde{v}$	1

Table 1: Walker's decision process. Firstly walkers change the direction of movement and, afterwards, they modify their speed in probability. Finally, walkers who are close to a wall, reduce the velocity normal component linearly with the distance from the wall at constant speed. Square brackets denote functional dependence.

where the velocity has been decomposed in speed and direction $\boldsymbol{v} = \{v, \theta\}$. Three types of stimuli are assumed to contribute to the modification of walking direction, namely, the desire to reach a defined target, the attraction toward the mean stream and the attempt to avoid overcrowded areas. These are represented by the three unit vectors $\boldsymbol{\nu}^{(t)}$, $\boldsymbol{\nu}^{(s)}$ and $\boldsymbol{\nu}^{(v)}$, respectively. It is expected that the at high density, walkers try to drift apart from the more congested area moving in the direction of $\boldsymbol{\nu}^{(v)}$. Conversely, at low density, walkers head for the target identified by $\boldsymbol{\nu}^{(t)}$ unless their level of anxiety is high in which case they tend to follow the mean stream as given by $\boldsymbol{\nu}^{(s)}$.

Accordingly, the preferred direction is defined as

$$\boldsymbol{\nu}^{(p)} = \frac{\tilde{\rho}\boldsymbol{\nu}^{(v)} + (1-\tilde{\rho})\,\dfrac{\beta\boldsymbol{\nu}^{(s)} + (1-\beta)\boldsymbol{\nu}^{(t)}}{\|\beta\boldsymbol{\nu}^{(s)} + (1-\beta)\boldsymbol{\nu}^{(t)}\|}}{\left\|\tilde{\rho}\boldsymbol{\nu}^{(v)} + (1-\tilde{\rho})\,\dfrac{\beta\boldsymbol{\nu}^{(s)} + (1-\beta)\boldsymbol{\nu}^{(t)}}{\|\beta\boldsymbol{\nu}^{(s)} + (1-\beta)\boldsymbol{\nu}^{(t)}\|}\right\|}, \tag{6}$$

where $\tilde{\rho} = \rho/\rho_{\text{MAX}}$, being ρ_{MAX} the highest admissible packing density, and

$$\boldsymbol{\nu}^{(v)} = -\frac{\nabla_{\boldsymbol{x}}\rho}{\|\nabla_{\boldsymbol{x}}\rho\|}, \qquad \boldsymbol{\nu}^{(s)} = \frac{\boldsymbol{\xi}}{\|\boldsymbol{\xi}\|} \tag{7}$$

In Eq. (6), $\beta \in [0,1]$ is a parameter which models the sensitivity to the stream with respect to the search of vacuum and it is supposed measured, to some extent, the level of anxiety of walkers.

The transition probabilities for angles is thus defined

$$\mathcal{C}_1[\rho, \boldsymbol{\xi}](\theta_* \to \tilde{\theta}) = \delta\left(\tilde{\theta} - \theta^{(p)}\right) \tag{8}$$

where the preferred angle of motion, $\theta^{(p)}$, is obtained from Eq. (6) through the relation $\boldsymbol{\nu}^{(p)} = (\cos\theta^{(p)}, \sin\theta^{(p)})$.

For what speed is concerned, we first introduce the perceived density along the direction $\theta^{(p)}$ which reads

$$\rho_p = \rho_p[\rho] = \rho + \frac{\partial_p\rho}{\sqrt{1+(\partial_p\rho)^2}}\left[(\rho_{\text{MAX}} - \rho)\,H(\partial_p\rho) + \rho\,H(-\partial_p\rho)\right], \tag{9}$$

where ∂_p denotes the derivative along the direction $\theta^{(p)}$ while $H(\cdot)$ is the Heaviside function $H(\cdot \geq 0) = 1$, and $H(\cdot < 0) = 0$. According to Eq. (9) it results

$$\partial_p\rho \to \infty \Rightarrow \rho_p \to \rho_{\text{MAX}}\,, \quad \partial_p\rho = 0 \Rightarrow \rho_p = \rho\,, \quad \partial_p\rho \to -\infty \Rightarrow \rho_p \to 0\,.$$

Bearing all above in mind, two cases are distinguished:

- The walker's speed is greater or equal than the mean speed. The walker either maintains its speed, if for instance there is enough space to overtake the leading walker, or decelerate to a speed ξ_d which is as much lower as the higher is the density. It is reasonable to assume that the probability to decelerate, p_d, increases with the congestion of the space, the badness of the environmental condition and the anxiety level of the walker measured by the parameters α and β, respectively.

- The walker's speed is lower than the mean speed. The walker either maintains its speed or accelerate to a speed ξ_a which is as much higher as the lower is the density, the higher is the gap between the mean speed and the preferred speed and the goodness are the environmental conditions. It is reasonable to assume that the probability to accelerate, p_a, decreases with the congestion of the space and with the badness of the environmental condition and the anxiety level of the walker.

Accordingly the transition probability density for the speed reads

$$\mathcal{C}_2[\rho, \boldsymbol{\xi}](v_* \to \tilde{v}) = \{p_a \delta(\tilde{v} - \xi_a) + (1 - p_a)\,\delta(\tilde{v} - v_*)\}\, H(\xi - v_*) \\ \{p_d \delta(\tilde{v} - \xi_d) + (1 - p_d)\,\delta(\tilde{v} - v_*)\}\, H(v_* - \xi)\,, \quad (10)$$

where, by denoting $\tilde{\rho_p} = \rho_p / \rho_{\mathrm{MAX}}$,

$$\xi_d = \xi - \tilde{\rho_p}\xi, \qquad p_d = (1 - \gamma C)\tilde{\rho_p}, \quad (11)$$

and

$$\xi_a = \xi + \gamma(1 - \tilde{\rho_p})(\gamma\xi_{\mathrm{LIM}} - \xi), \qquad p_a = \gamma(1 - \tilde{\rho_p}). \quad (12)$$

In Eqs. (11) and (12), $\gamma = \alpha\beta$ where the parameter α measures the quality of the area in which the crowd is located and the constant $C < 1$ has been

introduced so as to take into account that the probability to decelerate is not naught even if $\gamma = 1$.

2.2. Modeling interactions with walls

The most important feature to be taken into account in modeling the interactions between walkers and walls is its non locality, as walkers are not classical particles and modify their velocity before encountering the wall. Following Ref. [8], we assume that walkers whose distances from the wall, d, are within a specified cutoff, d_w, modify their velocity $\tilde{\boldsymbol{v}}$ to a new velocity $\boldsymbol{v}^{(w)}$, by reducing the normal component linearly with the distance from the wall but keeping the speed constant, that is

$$\boldsymbol{v}^{(w)} = \frac{d}{d_w} \left(\tilde{\boldsymbol{v}} \cdot \boldsymbol{n}\right) \boldsymbol{n} + \mathrm{sign}(\tilde{\boldsymbol{v}} \cdot \boldsymbol{t}) \left[\tilde{v}^2 - \frac{d^2}{d_w^2} \left(\tilde{\boldsymbol{v}} \cdot \boldsymbol{n}\right)^2\right]^{1/2} \boldsymbol{t}, \tag{13}$$

where $\boldsymbol{n}$ and $\boldsymbol{t}$ are the normal and tangent to the wall.
The transition probability density $\mathcal{B}$ is then defined as

$$\mathcal{B}(\tilde{\boldsymbol{v}} \to \boldsymbol{v}) = \delta\left(\theta - \theta^{(w)}\right) \delta\left(v - v^{(w)}\right), \tag{14}$$

where $v^{(w)} = \tilde{v}$ and $\theta^{(w)}$ is the direction of the velocity $\boldsymbol{v}^{(w)}$ defined by Eq. (13) through the relation $\theta^{(w)} = \boldsymbol{v}^{(w)}/v^{(w)} = (\cos\theta^{(w)}, \sin\theta^{(w)})$.

3. Validation by fundamental diagrams

The experimental study on crowd behavior is not developed as widely as the analogous field of vehicular traffic flows. Nevertheless, some empirical data have been reported in the literature, often in the form of speed and flow fundamental diagrams, see for instance Refs. [10–13].

The density-speed diagram provides the mean speed of walkers as a function of the local mean density in homogeneous steady conditions. In free flow conditions, walkers move at the average maximum allowed speed which depends on the environmental conditions. Conversely, in congested flow conditions, walkers move closer to one another at a reduced speed, until the density reaches the jam density at which walkers stop and have zero speed.

It is worth stressing that the aforementioned diagram should not be artificially inserted into the equations of the model but rather be reproduced as a consequence of interactions at the microscopic scale. This is the approach followed in Ref. [14], where, starting from a statistical description of the microscopic interactions between vehicles, the fundamental diagrams of traffic flow have been obtained as stationary long-time asymptotic solutions of the corresponding kinetic equations. Likewise, we here show that, in the space-homogeneous case, the proposed model admits a closed form solution of the density-speed behavior.

We seek a one-dimensional, spatially and time independent solution in the form $f(t, \boldsymbol{x}, \boldsymbol{v}) = f^{(eq)}(v)$. Substituting this ansatz in Eq. (3) yields

$$0 = (1 + p_a) f^{(eq)}(v) H(\xi - v) + (1 - p_d) f^{(eq)}(v) H(v - \xi) + p_a \rho^{(-)} \delta(v - \xi_a) + p_d \rho^{(+)} \delta(v - \xi_d) - f^{(eq)}(v), \quad (15)$$

where the following notation has been introduced

$$\rho^{(-)} = \int_0^{\xi} f dv, \qquad \rho^{(+)} = \int_{\xi}^{\xi_{\text{LIM}}} f dv, \quad (16)$$

It is worth noticing that in the spatially homogeneous case the density ρ plays the role of a parameter fixed by the prescribed initial condition and

hence it can be regarded as a constant. Since Eq. (15) has to be satisfied for every v, the equilibrium distribution function must be of the form

$$f^{(eq)}(v) = \frac{p_a}{p_d}\rho^{(-)}\delta(v-\xi_a) + \frac{p_d}{p_a}\rho^{(+)}\delta(v-\xi_d). \tag{17}$$

Integrating Eq. (17) with respect to the velocity variable in the intervals $[0,\xi]$ and $[\xi,\xi_{\text{LIM}}]$ and using the fact that $\rho = \rho^{(-)} + \rho^{(+)}$, after some algebra we get

$$\rho^{(-)} = \frac{p_d}{p_d+p_a}\rho, \qquad \rho^{(+)} = \frac{p_a}{p_d+p_a}\rho. \tag{18}$$

Substituting Eqs. (18) into Eq. (17), the following equilibrium distribution function is obtained

$$f^{(eq)}(v) = \frac{p_a}{p_d+p_a}\rho\,\delta(v-\xi_a) + \frac{p_d}{p_d+p_a}\rho\,\delta(v-\xi_d). \tag{19}$$

Multiplying Eq. (19) by v and integrating with respect to the velocity variable, we get a linear system in the mean velocity which can be easily solved to give

$$\frac{\xi}{\xi_{\text{LIM}}} = \frac{\gamma^3\left(\rho_{\text{MAX}}-\rho\right)^2}{\gamma^2\left(\rho_{\text{MAX}}-\rho\right)^2 + (1-\gamma C)\,\rho^2} \tag{20}$$

It is worth noticing that Eq. (19) depends on the single parameter $\gamma = \alpha\beta$ which encompasses the quality of the venue, α, and the trend of walkers to imitate their surroundings instead of searching less crowded areas, β.

The fundamental diagram as provided by Eq. (20) is shown in Fig. 1. The mean features of the empirical evidence about the relation between density and velocity in a crowd are correctly reproduced. More specifically, the mean velocity of the walkers decreases monotonically with the density from the maximal value for $\rho = 0$ to zero when $\rho \to 1$. Moreover, the maximal velocity observed at very low density increases with γ, that is with the quality

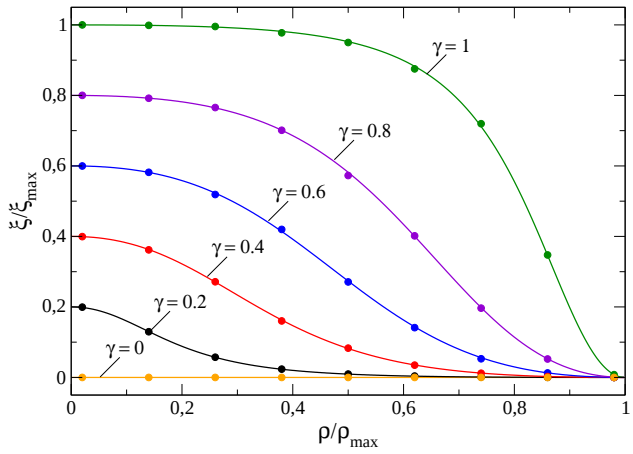

Figure 1: Fundamental diagram as a function of $\gamma = \alpha\beta$. Solid lines are the analytical solution as given by Eq. (20) with $C = 0.95$. Solid symbols are the numerical predictions obtained by the Monte Carlo method.

of the environmental conditions and/or the walkers' anxiety. The slope of the decay also depends on γ. Anxious walkers within high quality venues show a trend to keep the maximal velocity up to high densities while the mean velocity reduces more rapidly to zero in the opposite case.

4. Validation by emerging behaviors

A further validation of the proposed mesoscopic model is obtained by verifying that it can depict some emerging behaviors which are empirically observed. The comparison is developed at a qualitative level as these emerging behaviors often keep a qualitative shape but are quantitatively subject to deviations. Two specific case studies have been selected among various possible ones.

1. Self-organized lane formation: Walkers moving in opposite directions

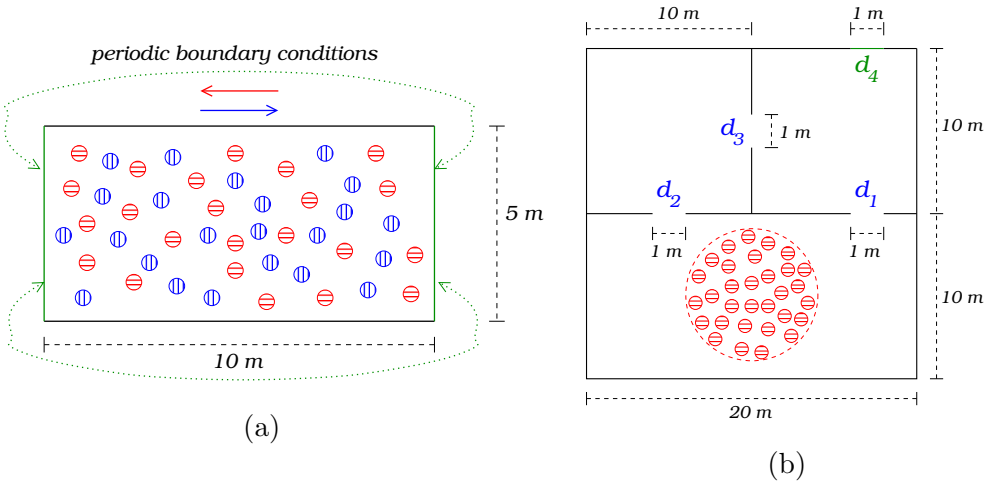

Figure 2: Case studies: (a) Pedestrian counterflow in a narrow street and (b) Evacuation from a complex venue.

tends to organize their movement into a number of dynamically varying lanes.

2. Evacuation from a complex venue: It is expected that the time elapsed between the instant that walkers receive the warning to evacuate and their arrival at destination increases under panic condition.

Subsection 4.1 briefly discuss the Monte Carlo method which has been used to obtain numerical solutions of the proposed kinetic model while a detailed discussion of these two case studies are contained in Subsections 4.2 and 4.3, respectively.

4.1. Sketch of the numerical method

The numerical simulations discussed in the following subsections have been carried out by using a particle method which closely resemble the Direct Simulation Monte Carlo (DSMC) scheme [15]. The latter is by far the most

popular and widely used simulation method in rarefied gas dynamics (see Refs. [16, 17] for recent applications to vacuum technology). Compared to alternative approaches, the proposed method of solution permits to easily handle venues with complex geometries while keeping the computing effort requirements at a reasonable level.

The basic idea is to represent the distribution function by a collection of computational particles whose positions and velocities evolve in time by a sequence of time steps, each of them consisting of a free flight and a local collision sub-steps. The former corresponds to the streaming operator on left hand-side of Eq. (3), whereas the latter is performed according to stochastic rules, consistent with the structure of the collision terms on the right-hand side of Eq. (3) and the transition probability densities given by Eqs. (8), (10) and (14). The space domain to be simulated is covered by a mesh of cells. These cells are used to collect together particles that may collide and also for the sampling of macroscopic properties such as density and mean velocity.

The numerical code is assessed by solving Eq. (3) in the space homogeneous case so as to verify to that the mean velocity given by Eq. (20) is reproduced. The distribution function at time $t = 0$ is assumed to be a delta function centered about $v = 0$ and the equation is integrated in time until a stationary state is reached. Figure 1 shows an excellent agreement between the numerical predictions and the known analytical solution.

4.2. Self-organized lanes formation

Simulations are carried out for two groups of walkers moving in opposite directions in a narrow street. Beside describing the segregation of walkers into lanes of uniform walking direction, the influence of the parameter β on

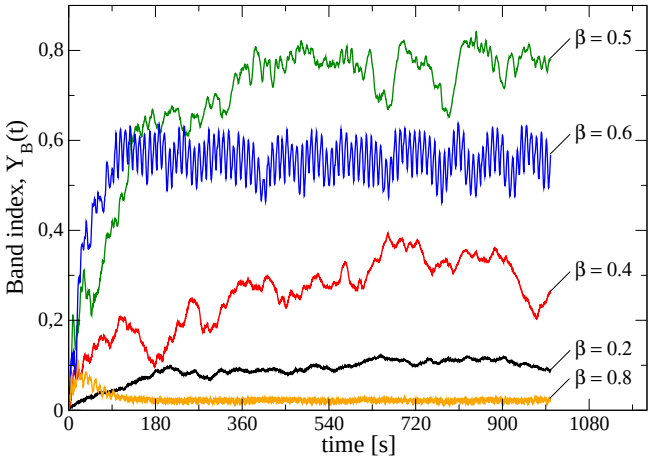

Figure 3: Band index of the density field related to the counterflow of a crowd composed by 50 walkers for different β.

the overall dynamics is assessed. A sketch of the initial conditions and of the geometry of the venue is shown in Fig. 2a. The crowd is composed by 50 walkers who are uniformly distributed in the domain.

The spontaneous formation of parallel lanes can be quantitatively assessed by computing the band index, $Y_{\rm B}(t)$, which measures the segregation of opposite flow directions [8, 18] and reads

$$Y_{\rm B}(t) = \frac{1}{L_x L_y} \int_0^{L_x} \left| \int_0^{L_y} \frac{\tilde{\rho}_1(t,\boldsymbol{x}) - \tilde{\rho}_2(t,\boldsymbol{x})}{\tilde{\rho}_1(t,\boldsymbol{x}) + \tilde{\rho}_2(t,\boldsymbol{x})}\, dx \right| dy\,, \tag{21}$$

where $\tilde{\rho}_1 = \rho_1/\rho_{\rm MAX}$ and $\tilde{\rho}_2 = \rho_2/\rho_{\rm MAX}$ are the normalized densities of the two groups of walkers. According to its definition, one has $Y_{\rm B}(t) = 0$ for mixed counter flows and $Y_{\rm B}(t) = 1$ for a perfect segregation of the opposite flows. As shown in Fig. 3, the long-time value of the band index is a non-monotonic function of β and the emergence of the spatial segregation is anticipated to be more pronounced for $\beta = 0.5$. By contrast, for higher values of β the self-organization pattern is expected to disappear with the walkers randomly

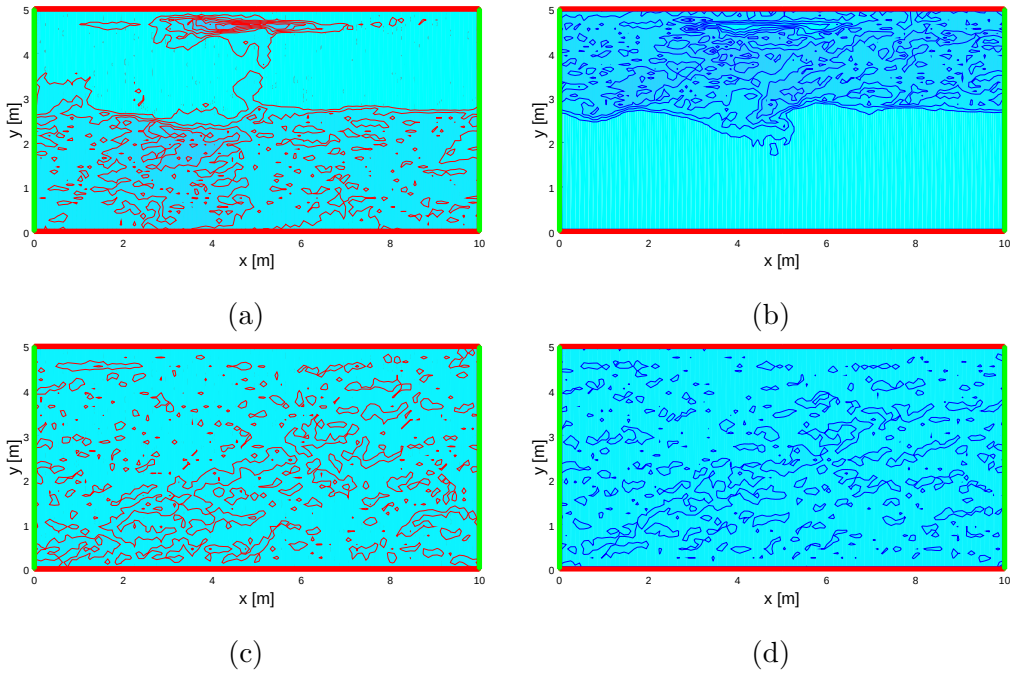

Figure 4: Density contour plot, ρ/ρ_{MAX}, of a crowd composed by 50 walkers divided into two groups which move leftward and rightward. These groups are represented, respectively, in panels (a) and (b) for $\beta = 0.5$, and in panels (c) and (d) for $\beta = 0.8$.

filling the domain. These results are clearly shown in Fig. 4.

4.3. Evacuation from a complex venue

Simulations are carried out for a group of walkers who evacuate a complex venue. The aim is not only to show that the proposed model provides a reasonable description of the crowd behavior, but also to verify that the evacuation time increases under panic conditions. A sketch of the initial conditions and of the geometry of the venue is shown in Fig.2b. The venue is made up of three rooms, which are connected by doors d_1, d_2 and d_3, while the exit is located in the upper right corner at door d_4. It is supposed that

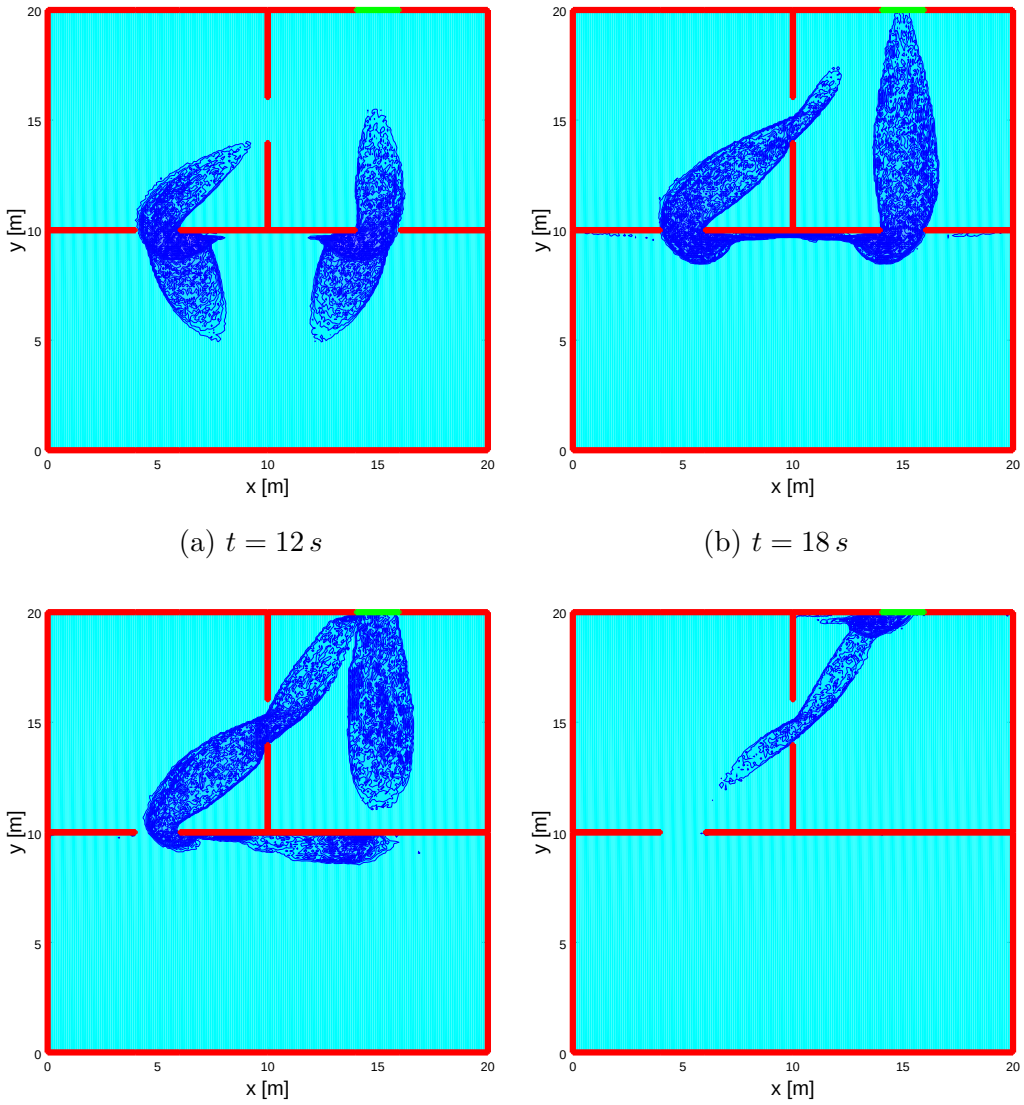

(a) $t = 12\,s$ (b) $t = 18\,s$

(c) $t = 24\,s$ (d) $t = 50\,s$

Figure 5: Density contour plot, ρ/ρ_{MAX}, of 50 walkers evacuating the venue with $\beta = 0.5$ at different instants of time.

the door d_1, due at to an incident, suddenly closes at $t = 20s$. The crowd is composed by 50 walkers who are located in the first room, at rest and

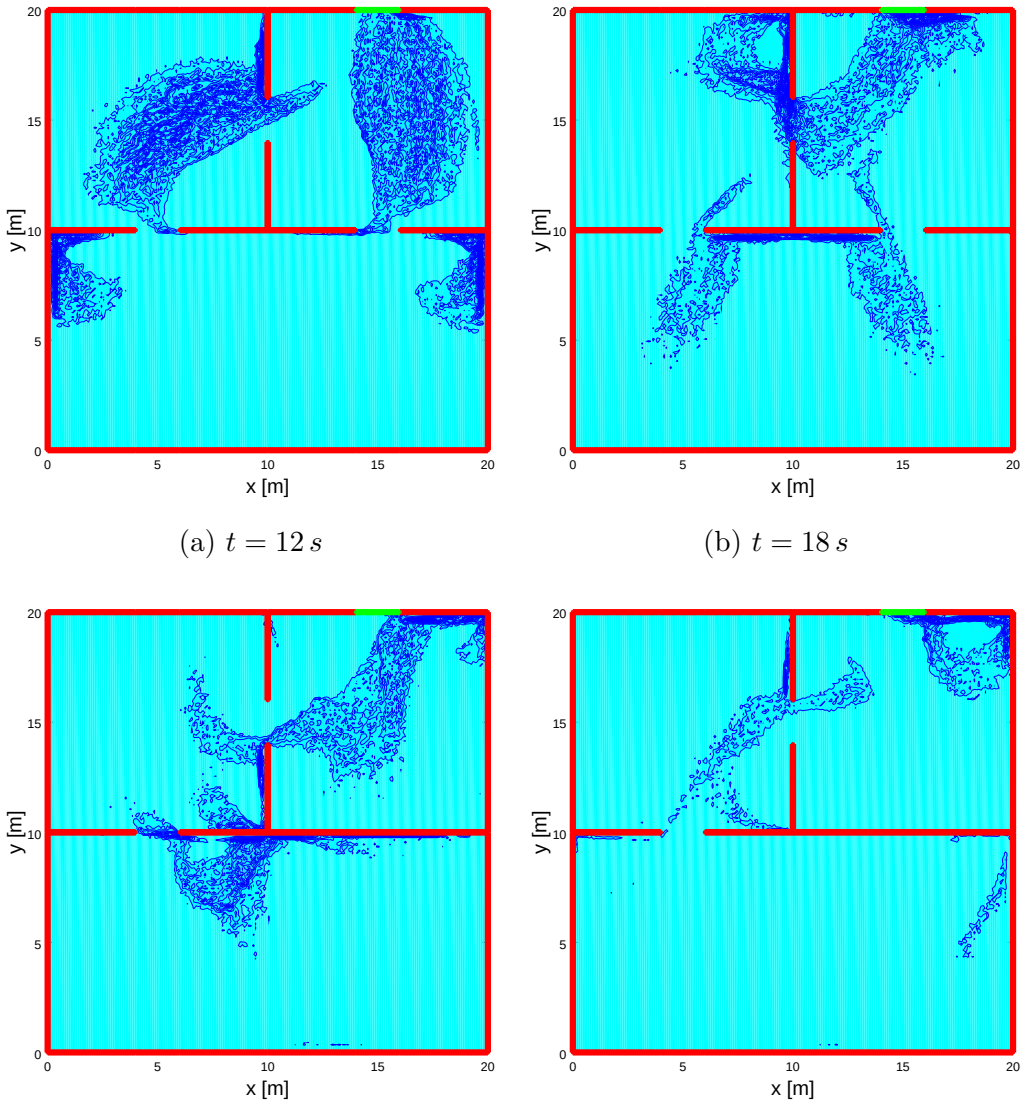

(a) $t = 12\,s$ (b) $t = 18\,s$

(c) $t = 24\,s$ (d) $t = 50\,s$

Figure 6: Density contour plot, ρ/ρ_{MAX}, of 50 walkers evacuating the venue with $\beta = 0.8$ at different instants of time.

uniformly distributed in a circular region of radius $4\,m$.

Fig. 5 shows the crowd dynamics for $\beta = 0.5$. As shown in Fig. 5a,

the original group symmetrically divides into two groups moving toward the closest between the doors d_1 and d_2. Figure 5b shows that only a part of the walkers succeed in passing door d_1 before it suddenly closes at $t = 20s$. Walkers who did not get through it, are obliged to change direction and move to door d_2 in the attempt to reach door d_4. The final stages of the dynamics are reported in Figs. 5c and 5d. Figures 6a-d display the same time sequence with parameter $\beta = 0.8$. It is quite evident that in this case the spatial distribution of walkers is less ordered as shown by density patterns.

Safety issues are likely to arise when walkers forget about looking for less congested areas and exhibit an uncritical directional consensus. This aspect can be highlighted by computing the time needed to exit the venue for different values of β.

Figure 7 shows the number of walkers in the venue as a function of time for different values of β. It is apparent that the evacuation time initially decreases which is not unexpected since the higher is β the lower is the mean velocity as it results from Eq. (20). However, this is not any more the case for $\beta = 0.8$. Indeed at time $t = 50s$, the number of walkers in the venue are less than 5 for $\beta = 0.6$ but increases to more than 15 for $\beta = 0.8$. The reason for this behavior is twofold. Firstly, when β approaches the value 1 the walkers' movement becomes more and more erratic since the stimulus to get to the target reduces. Secondly, area with high density arise from the dynamics as walkers tend to do what the others do. This, in turn, increases the congestion level and therefore reduces the local mean velocity.

5. Conclusion

This paper has revisited the mesoscopic crowd model proposed in Ref. [8] with the aim to simplify its mathematical formulation and, at the same time, to improve its capability to reproduce the available empirical evidence.

A two-steps validation strategy has been been pursued to assess the proposed model. Firstly, it has been analytically verified that, in the space-homogeneous case, a fundamental density-velocity diagram is obtained whose features are consistent with those empirically observed. Secondly, it has been numerically shown that, in the space-nonhomogeneous case, well known emerging properties are reproduced, such as lane formation in pedestrian counter flow and the increasing of the evacuation time under panic conditions. It is worth pointing out that these features have not been inserted artificially into the model but they are consequences of the dynamics at the microscopic scale.

Furthermore the proposed model has turned out to be amenable to an efficient numerical treatment based on a Monte Carlo particle method of solution which has made feasible the study of crowd behavior in a relatively complex venue with a time-varying geometry. The present paper can thus be considered the first step towards the development of a simulation tool which can meet the practical needs of crowd dynamics applications.

Future research directions, selected according to the authors' bias, can be outlined from this paper.

The derivation of macroscopic models from the underlying description at the microscopic scale can be carried out according to an approach recently applied to derive hydrodynamic models of vehicular traffic [19] and human

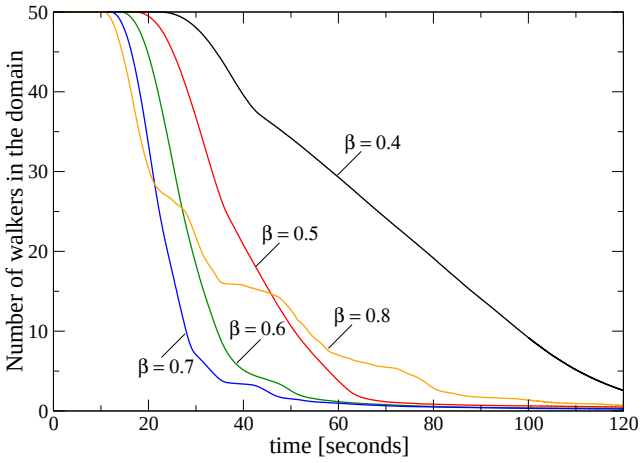

Figure 7: Number of walkers in the venue as a function of time for different β.

crowd [20]. Both results were obtained in the relatively simple case of flows in unbounded domains, where the result required the *a priori* heuristic assumption of existence of an equilibrium solution. This paper offers additional tools to develop micro-macro derivation within a more general framework.

It is worth stressing that the derivation of macroscopic models by the classical heuristic approach needs the modeling of the velocity selected by the walkers [4]. This aspect has been only tangentially treated for first-order models in Ref. [21] and for second-order models in Ref. [22]. The present paper provides a criterion to model local velocity which has been partially developed in Ref. [23], although additional work is still needed.

A further topic worth to be studied is the propagation of social behaviors, which can be transferred across individuals due to their ability to communicate. The modeling of such process poses additional difficulties in that it needs linking mechanical movement to learning and social dynamics, see Refs. [24] and [25]. This challenging issue will be subject of a forthcoming

paper.

Acknowledgement

The research leading to these results has received funding from the European Unions Seventh Framework Programme (FP7/20072013) under Grant Agreement Number 313161 (eVACUATE). Project title: "A holistic, scenario independent, situation-awareness and guidance system for sustaining the Active Evacuation Route for large crowds". This publication reflects the views only of the authors and the Commission cannot be held responsible for any use which may be made of the information here contained.

References

[1] N. Bellomo and C. Dogbè. On the modeling of traffic and crowds: A survey of models, speculations, and perspectives. *Siam review*, 53(3):409–463, 2011.

[2] E. Cristiani, B. Piccoli, and A. Tosin. *Multiscale Modeling of Pedestrian Dynamics*. Springer, 2014.

[3] D. Helbing. Traffic and related self-driven many-particle systems. *Review of Modern Physics*, 73(4):1067–1141, 2001.

[4] R.L. Hughes. The flow of human crowds. *Annual Review of Fluid Mechanics*, 35:169–182, 2003.

[5] N. Bellomo, D. Knopoff, and J. Soler. On the difficult interplay between life, "complexity", and mathematical sciences. *Mathematical Models and Methods in Applied Sciences*, 23(10):1861–1913, 2013.

[6] R. Borsche, A. Klar, S. Köhn, and A. Meurer. Coupling traffic flow networks to pedestrian motion. *Mathematical Models and Methods in Applied Sciences*, 24(2):359–380, 2014.

[7] N. Bellomo, A. Bellouquid, and D. Knopoff. From the micro-scale to collective crowd dynamics. *Multiscale Models & Simulation*, 11(3):943–963, 2013.

[8] N. Bellomo and L. Gibelli. Toward a behavioral-social dynamics of pedestrian crowds. *Mathematical Models and Methods in Applied Sciences*, 25(13):2417–2437, 2015.

[9] D. Helbing, A. Johansson, and H.Z. Al-Abideen. Dynamics of crowd disasters: An empirical study. *Physical Review E*, 75(4):046109, 2007.

[10] A. Schadschneider, W. Klingsch, H. Kläpfel, T. Kretz, C. Rogsch, and A. Seyfried. *Encyclopedia of Complexity and System Science*, chapter Evacuation Dynamics: Empirical Results, Modeling and Applications, pages 3142–3176. Springer, 2009.

[11] A. Schadschneider and A. Seyfried. Empirical results for pedestrian dynamics and their implications for modeling. *Network and Heterogeneous Media*, 6:545–560, 2011.

[12] W. Daamen and S.P. Hoogedorn. Trb annual meeting cd-rom, 2006. Springer.

[13] A. Seyfried, B. Steffen, W. Klingsch, Th. Lippert, and M. Boltes. The fundamental diagram of pedestrian movement revisited - empirical results and modelling. In Andreas Schadschneider, Reinhart Kühne,

Thorsten Pöschel, Michael Schreckenberg, and Dietrich E. Wolf, editors, *Traffic and Granular Flow 2005*. Springer, Berlin, 2006.

[14] L. Fermo and A. Tosin. Fundamental diagrams for kinetic equations of traffic flow. *Mathematical Models and Methods in Applied Sciences*, 7(3):449–462, 2014.

[15] G.A. Bird. *Molecular gas dynamics and the direct simulation of gas flows*. Oxford University Press, 1994.

[16] A. Frezzotti, G.P. Ghiroldi, and L. Gibelli. Rarefied gas mixtures flows driven by surface absorption. *Vacuum*, 86(11):1731–1738, 2012.

[17] A. Frezzotti, G.P. Ghiroldi, L. Gibelli, and Bonucci. Dsmc simulation of rarefied gas mixtures flows driven by arrays of absorbing plates. *Vacuum*, 103:57–67, 2014.

[18] Y. Yamori. Going with the flow: Micro-macro dynamics in the macrobehavioral patterns of pedestrian crowds. *Psychological Review*, 105(3):530–557, 1998.

[19] N. Bellomo, A. Bellouquid, J. Nieto, and J. Soler. On the multiscale modeling of vehicular traffic: From kinetic to hydrodynamics. *Discrete and Continuous Dynamical Systems Series B*, 19(7):1869–1888, 2014.

[20] N. Bellomo and A. Bellouquid. On multiscale models of pedestrian crowds from mesoscopic to macroscopic. *Communications in Mathematical Sciences*, 13(7):1649–1664, 2015.

[21] V. Coscia and C. Canavesio. First order macroscopic modelling of human crowd dynamics. *Mathematical Models and Methods in Applied Sciences*, 18(1):1217–1247, 2008.

[22] N. Bellomo and C. Dogbè. On the modelling crowd dynamics from scaling to hyperbolic macroscopic models. *Mathematical Models and Methods in Applied Sciences*, 18:1317–1345, 2008.

[23] N. Bellomo, S. Berrone, L. Gibelli, and A.B. Pieri. First-order models of multicomponent human crowds with behavioral dynamics. In K. Takizawa and Y. Bazilevs, editors, *Advances in Computational Fluid-Structure*. Bïrkhauser, 2015.

[24] D. Burini, S. De Lillo, and L. Gibelli. Collective learning modelling based on the kinetic theory of active particles. Accepted for publication in Physics of Life Reviews.

[25] G. Ajmone Marsan, N. Bellomo, and L. Gibelli. Towards a systems approach to behavioral social dynamics. *Mathematical Models and Methods in Applied Sciences*, 26(to appear), 2016.